

CMB limits on large-scale magnetic fields in an inhomogeneous universe

C. A. Clarkson^{1,2}, A. A. Coley¹, R. Maartens³, C. G. Tsagas^{3,2}

¹ Department of Mathematics & Statistics, Dalhousie University, Halifax B3H 3J5, Canada

² Relativity & Cosmology Group, Department of Mathematics & Applied Mathematics, University of Cape Town, Cape Town 7701, South Africa

³ Institute of Cosmology & Gravitation, University of Portsmouth, Portsmouth PO1 2EG, UK

Abstract.

We use the cosmic microwave background temperature anisotropy to place limits on large-scale magnetic fields in an inhomogeneous (perturbed Friedmann) universe. If no assumptions are made about the spacetime geometry, only a weak limit can be deduced directly from the CMB. In the special case where spatial inhomogeneity is neglected to first order, the upper limit is much stronger, i.e. a few $\times 10^{-9}$ G.

1. Introduction

Magnetic fields have been observed in the universe on a wide range of scales. Fields with strengths of a few μ G are prolific in galaxies and galaxy clusters, extending well beyond the core regions of the latter, and have also been detected in high redshift Lyman- α objects (see [1] for recent reviews). These fields are the result of amplification of seed fields during structure formation, by adiabatic compression or by the dynamo mechanism. On scales above a significant fraction of the Hubble length, a magnetic field could not arise from structure formation, but would have to be a primordial field, redshifting with expansion:

$$B = B_0 \left(\frac{a_0}{a} \right)^2, \quad (1)$$

where B_0 is the current field strength.

The strength of primordial, cosmological magnetic fields is limited by observed helium abundances and by the near-isotropy of the cosmic microwave background (CMB) (see [1]). A magnetic field present at nucleosynthesis adds to the relativistic energy density, increasing the expansion rate so that the neutron-proton freeze out of weak interactions occurs at a higher temperature. The result is an increase in the abundance of primordial helium. Then 4 He observations (extrapolated to zero metallicity) provide an upper limit, which turns out to be $B_0 \lesssim 10^{-7}$ G.

A magnetic field generates anisotropy in radiation, and stronger limits on B_0 arise from the observed near-isotropy of the CMB. The COBE data place an upper bound on a homogeneous magnetic field present at the time of last scattering. In a recent analysis of a particular class of spatially homogeneous Bianchi universes, an upper bound of $B_0 \lesssim 10^{-9}$ G was obtained [2]. Here we generalize previous work to the case of inhomogeneous fields in an inhomogeneous almost-Friedmann universe. We also generalize the limits found in [2] by weakening some of their assumptions. It turns out that, if we do not assume a spatially homogeneous geometry, the limits imposed directly by CMB data on super-Hubble magnetic fields in an inhomogeneous universe are much weaker, $B_0 \lesssim 10^{-6}$ G. A similar situation arises when considering the limits placed on the shear by CMB anisotropies, as pointed out in [3].

Recently it was proven [4] under quite general circumstances that a magnetic field is prohibited in spacetimes where exactly isotropic radiation is also present. Taking this as our starting point, small

anisotropy allows for a weak magnetic field. We use the 1+3-covariant analysis of CMB temperature anisotropies [5, 6, 7] and of magnetic fields [8], in order to derive limits on large-scale fields as a function of coherence scale. Following the approach of [6, 9], we use the radiation multipoles to derive limits which are model-independent, in the sense that they do not rely on assumptions about the (perturbed Friedmann) spacetime geometry.

In Sec. 2 we outline the general formalism for imposing limits on large-scale magnetic fields from observed CMB temperature anisotropies. In Sec. 3, we give our main results, which follow from a refinement of the method in [9]. For convenience, we omit most of the calculational details, and give the key equations in Appendices A and B. We use units such that $8\pi G = 1 = c$. Our notation follows that of [10]. In particular, $\dot{X}_{a\cdots b} = u^c \nabla_c X_{a\cdots b}$ and D_a is the covariant derivative in the rest space, i.e., $D_c X_{a\cdots b} = h_c^d h_a^e \cdots h_b^f \nabla_d X_{e\cdots f}$, where $h_{ab} = g_{ab} + u_a u_b$ is the projection tensor. Angled brackets on indices denote the projected, symmetric and trace free (PSTF) part. The 3-divergence and 3-curl of PSTF tensors are $\text{div } X_a = D^b X_{ab}, \dots$, and $\text{curl } X_a = \varepsilon_{abc} D^b X^c, \text{curl } X_{ab} = \varepsilon_{cd(a} D^c X_{b)}^d, \dots$.

2. CMB anisotropy induced by large-scale magnetic fields

In the 1+3-covariant analysis of CMB anisotropy [6, 7], a physical choice of 4-velocity u^a is made, usually the 4-velocity of cold dark matter (CDM), and all perturbative quantities are then covariant vectors or tensors in the rest-space of u^a , with direct geometrical or physical meaning. The fractional temperature fluctuation is expanded in covariant multipoles τ_{A_ℓ} ($A_\ell = a_1 \cdots a_\ell$), which are PSTF tensors. These are limited directly by observations:

$$|\tau_{A_\ell}| \equiv \sqrt{\tau_{A_\ell} \tau^{A_\ell}} < \epsilon_\ell. \quad (2)$$

COBE data leads to the values [11]

$$\epsilon_2 \approx 1.1(\pm 0.8) \times 10^{-5}, \quad (3)$$

$$\epsilon_3 \approx 2.5(\pm 1.3) \times 10^{-5}, \quad (4)$$

which we use here. The first moment τ_a is the dipole, which is usually attributed to our peculiar motion relative to the CMB frame. We assume this motion is corrected for by setting $\tau_a = 0 = \epsilon_1$ for the bulk of the paper. However, it is possible that a residual dipole of cosmological origin exists (it would be frequency dependent, and thus could not be set to zero by a Lorentz boost), and we include it in our calculations for generality.

In addition to the observed bounds on the τ_{A_ℓ} , we need bounds on their temporal and spatial gradients, in order to find limits on geometrical and physical quantities that characterize the spacetime. We define the expansion-normalized, dimensionless ϵ -quantities [6, 9]

$$\begin{aligned} |\dot{\tau}_{A_\ell}| &< 3H\epsilon_\ell^*, \quad |\ddot{\tau}_{A_\ell}| < 9H^2\epsilon_\ell^{**}, \quad \dots, \\ |D_a \tau_{A_\ell}| &< 3H\epsilon_\ell^\dagger, \quad |D_a D_b \tau_{A_\ell}| < 9H^2\epsilon_\ell^{\dagger\dagger}, \quad \dots, \\ |(D_a \tau_{A_\ell})'| &< 9H^2\epsilon_\ell^{\dagger*}, \quad |(D_a D_b \tau_{A_\ell})'| < 27H^3\epsilon_\ell^{\dagger\dagger*}, \quad \dots, \end{aligned} \quad (5)$$

where H is the background Hubble rate.

Following [9], we can find upper bounds on all perturbative quantities in terms of the ϵ_ℓ , ϵ_ℓ^* , ϵ_ℓ^\dagger , etc. However, the derivative bounds ϵ_ℓ^* , $\epsilon_\ell^\dagger \dots$ are not directly measurable, as we are unable to move a cosmological time- or space-separation from our current spacetime event. Here we make the simple assumption that the time- and space-variations of the multipoles are governed respectively by the Hubble rate and the physical scale λ of the perturbation, i.e.,

$$|\dot{\tau}_{A_\ell}| \sim H|\tau_{A_\ell}|, \quad |D_a \tau_{A_\ell}| \sim \frac{1}{\lambda}|\tau_{A_\ell}|. \quad (6)$$

This assumption implies

$$\epsilon_\ell^* \sim \frac{1}{3}\epsilon_\ell, \quad \epsilon_\ell^{**} \sim \frac{1}{9}\epsilon_\ell, \quad \dots, \quad (7)$$

$$\epsilon_\ell^\dagger \sim \frac{1}{3\beta}\epsilon_\ell, \quad \epsilon_\ell^{\dagger\dagger} \sim \frac{1}{9\beta^2}\epsilon_\ell, \quad \dots \quad \text{where } \beta = \frac{\lambda}{H^{-1}}. \quad (8)$$

The dimensionless parameter β gives the coherence scale as a fraction of the Hubble length, with $\beta \gtrsim O(1)$ since we are considering large scales.

The magnetic field is ‘frozen’ into the baryonic fluid, which may be treated as an infinitely conducting medium. We neglect the velocity of CDM relative to baryons, since the calculations become intractable otherwise. Then we choose the 4-velocity u^a as the velocity of pressure-free CDM-plus-baryons, whose total density is ρ_M . The kinematics of the matter are characterized by the volume expansion Θ , rotation ω^a , acceleration A^a and shear distortion σ_{ab} of u^a . Even in the absence of pressure gradients, the flow lines are generally non-geodesic (i.e. $A_a \neq 0$) due to the magnetic field. Here, however, we assume that the field is too weak to affect the motion of the baryonic matter; we impose the force-free condition on the magnetic field (i.e. $\epsilon_{abc} B^b \text{curl} B^c = 0$), which implies that the acceleration vanishes to first order.

The energy-momentum tensor of the magnetized dust is

$$T_{ab} = (\rho_B + p_B)u_a u_b + p_B h_{ab} + \Pi_{ab}, \quad (9)$$

where $\rho_B = B^2/8\pi$ and $p_B = \rho_B/3$ are the magnetic energy density and isotropic pressure respectively. The magnetic anisotropic stress is $\Pi_{ab} = -B_{\langle a} B_{b\rangle}/4\pi$. The radiation energy-momentum tensor is

$$T_{ab} = \mu u_a u_b + \frac{1}{3}\mu h_{ab} + 2u_{(a} q_{b)} + \pi_{ab}, \quad (10)$$

where μ , q_a and π_{ab} are the photon energy density, momentum density and anisotropic stress. These are directly related to the temperature anisotropy multipoles by [6]

$$q_a = \frac{4}{3}\mu\tau_a, \quad \pi_{ab} = \frac{8}{15}\mu\tau_{ab}. \quad (11)$$

The photon energy momentum tensor involves only the first two multipoles, but we will require also the octupole

$$\xi_{abc} = \frac{8}{35}\mu\tau_{abc}, \quad (12)$$

which appears in the evolution equation for π_{ab} , Eq. (A.7).

The field equations $G_{ab} = T_{ab} + \mathcal{T}_{ab}$, the Ricci identities and the Bianchi identities may be split into a set of evolution (along u^a) and constraint equations. The evolution of the magnetic field is determined by Maxwell’s equations. The reader is referred to Appendix A for the necessary equations.

3. The limits

We first present the CMB limits on inhomogeneous magnetic fields as a function of coherence scale, λ ; then we discuss the homogeneous case.

3.1. Inhomogeneous universe

Our procedure to find constraints on the magnetic field strength ρ_B , or equivalently $|\Pi_{ab}|$, is a generalization of the non-magnetized analysis in [9]. Briefly, we manipulate the field equations to express Π_{ab} in terms only of the radiation quantities $\mu, q_a, \pi_{ab}, \xi_{abc}$. This is facilitated by the appearance of the shear in Eq. (A.7), which, in the absence of acceleration, is the only coupling of the radiation to the first-order kinematical quantities. The main aspects of this calculation are in Appendix B, and the key result is Eq. (B.8).

Neglecting the dipole moment and the energy density of the radiation Ω_R , and restoring units, Eq. (B.8) gives

$$\begin{aligned} B_0 < \max(B) \equiv & \left(\frac{3}{2} \right)^{3/4} \frac{cH_0}{\sqrt{G}} \left\{ \frac{1}{4} \Omega_M \left(5\epsilon_2^* + \frac{45}{7}\epsilon_3^\dagger \right) + \Omega_\Lambda \left(\epsilon_2^* + \frac{9}{7}\epsilon_3^\dagger \right) \right. \\ & + 2\epsilon_2^* + \frac{15}{2}\epsilon_2^{**} + \frac{9}{2}\epsilon_2^{***} + 3\epsilon_2^{\dagger\dagger} + \frac{9}{2}\epsilon_2^{\dagger\dagger*} + \frac{81}{10}\epsilon_2^{\dagger\dagger\dagger} \\ & \left. + \frac{18}{7}\epsilon_3^\dagger + \frac{135}{14}\epsilon_3^{\dagger*} + \frac{81}{14}\epsilon_3^{\dagger**} + \frac{81}{14}\epsilon_3^{\dagger\dagger\dagger} \right\}^{1/2}, \end{aligned} \quad (13)$$

where the ϵ 's are evaluated at the current time. The function $\max(B)$ gives upper limits on large-scale magnetic fields, coherent on a given scale λ , imposed by CMB temperature anisotropies. This upper limit is given directly in terms of CMB multipoles and their derivatives, and is model-independent, i.e., no assumptions have been made about the spacetime geometry.

For a numerical estimate, we need to use the simple assumptions of Eqs. (7) and (8), in order to evaluate the derivative- ϵ 's. Then we find, in terms of the observable quantities ϵ_2, ϵ_3 , that

$$\begin{aligned} \max(B) = & \left(\frac{3}{2}\right)^{3/4} \frac{cH_0}{\sqrt{G}} \left\{ \epsilon_2 \left[\frac{5}{12}\Omega_M + \frac{1}{3}\Omega_\Lambda + \frac{5}{3} + \frac{1}{2}\beta^{-2} + \frac{1}{10}\beta^{-4} \right] \right. \\ & \left. + \epsilon_3 \left[\frac{1}{7} \left(\frac{5}{4}\Omega_M + \Omega_\Lambda + 5 \right) \beta^{-1} + \frac{3}{14}\beta^{-3} \right] \right\}^{1/2}. \end{aligned} \quad (14)$$

This is our main result. Using the limits in Eqs. (3) and (4), we can evaluate $\max(B)$, which is plotted in Fig. 1. One of the main features of the plot is that uncertainty in ϵ_2 and ϵ_3 from COBE data produces a far greater uncertainty than the uncertainty in the cosmological parameters.

On the largest scales, $\beta \rightarrow \infty$, Eq. (13) simplifies to give

$$\max(B)|_{\beta \rightarrow \infty} = \left(\frac{3}{2}\right)^{3/4} \frac{cH_0}{\sqrt{G}} \left\{ \frac{5}{12}\Omega_M + \frac{1}{3}\Omega_\Lambda + \frac{5}{3} \right\}^{1/2} \epsilon_2. \quad (15)$$

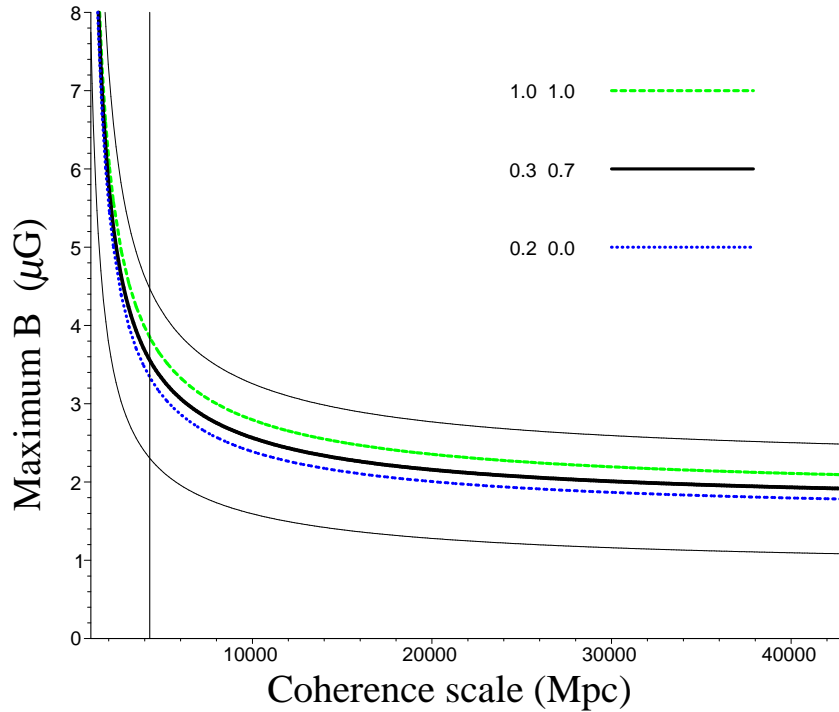


Figure 1. Maximum magnetic field strength in μG on large scales as a function of coherence scale λ ($\gtrsim 1000$ Mpc) for various cosmological parameters $\{\Omega_M, \Omega_\Lambda\}$ shown in the key, with $h = H_0/(100 \text{ km/s/Mpc}) = 0.7$. The concordance model $\{\Omega_M, \Omega_\Lambda\} = \{0.3, 0.7\}$ (central thick solid curve) is straddled on either side by the collective uncertainty in ϵ_2 and ϵ_3 (outer thin solid curves). An open and a closed model with extreme parameters are shown by the dashed curves, indicating how little the cosmological parameters affect the upper limit, and certainly much less than the observational uncertainty. The vertical line represents the Hubble distance, $\lambda = 3000h^{-1}$ Mpc.

3.2. Spatially homogeneous universe

The upper limit on B_0 on the largest scales in the general case of an inhomogeneous universe, as given by Eq. (15), is much weaker than the limit that can be imposed if we assume that the universe is spatially homogeneous to first order. Homogeneity implies that we can set to zero the ϵ 's that involve gradients, as we did in deriving Eq. (15).[‡] However, it is not only the radiation multipoles that are homogeneous to first order, but the whole spacetime, leading to a Bianchi model. The special dynamics of Bianchi models then leads to a tighter constraint on B_0 . A similar situation arises when deriving limits on the shear σ_{ab} [3].

It follows from [9] that the spatial 3-curvature vanishes to first order, $\mathcal{R}_{ab} = \mathcal{R} = 0$. In addition the shear becomes, from Eq. (A.7),

$$\sigma_{ab} = -\dot{\tau}_{ab}. \quad (16)$$

Thus the shear evolution equation becomes, using Eq. (A.18),

$$\Pi_{ab} = \ddot{\tau}_{ab} + \Theta\dot{\tau}_{ab} + \frac{8}{15}\mu\tau_{ab}. \quad (17)$$

The magnetic field acts as a forcing term for the quadrupole. The particular solution associated with this forcing term is

$$\Pi_{ab} = \frac{8}{15}\mu\tau_{ab}, \quad (18)$$

with $\dot{\tau}_{ab} = 0$ for the particular solution. The solution to the (non-magnetic) homogeneous part oscillates (at frequency $\approx \sqrt{8\mu/15}$), while being suppressed with a damping scale of the Hubble time. Thus a conservative upper limit is given by Eq. (18); using Eq. (4) and $\Omega_R \sim 2.5h^{-2} \times 10^{-5}\Omega_M$, we find that

$$B_0 < 6.2^{+1.9}_{-3.0} \times 10^{-9} \sqrt{\Omega_M} G. \quad (19)$$

With $\Omega_M = 0.3$, Eq. (19) gives

$$B_0 < 3.4^{+1.0}_{-1.6} \times 10^{-9} G. \quad (20)$$

This confirms the value found in [2], and is derived under slightly weaker assumptions; the spacetime is not chosen as a specific exact Bianchi model, but is homogeneous to first order, and turns out to be Bianchi I if we start with a flat Friedmann background. Furthermore, we include both the radiation energy density and the cosmological constant. In the set of Bianchi models which admit a pure magnetic field (types I, II, III, IV_o, VII_o), they are all of the same genericity; therefore we may consider this more general than [2], where the geometry is assumed to be type VII_h.

4. Conclusions

For large-scale magnetic fields in an inhomogeneous almost-Friedmann universe, we have found upper limits on the field strength directly in terms of the CMB temperature multipoles and their derivatives, as given by Eqs. (13) and (14). On super-Hubble scales, this upper limit is very weak:

$$B_0 \lesssim 2 \times 10^{-6} G$$

for the concordance model, as shown by Eq. (15) and Fig. 1.

When the almost-Friedmann universe is assumed to be homogeneous to first order, i.e. a Bianchi spacetime, the upper limit is much stricter, as given by Eq. (19). This generalizes the result of [2], by including a cosmological constant and removing initial assumptions of a choice of model.

These limits have been derived in a covariant and gauge invariant way using the 1+3 formalism. A major feature of our approach is that our limits are largely model-independent, being derived from properties of the Einstein-Boltzmann equations. Our main assumptions are imposed on the ϵ -quantities that bound the derivatives of radiation multipoles, which are in principle observable but in practice are not measurable.

It is also possible to find limits on the inhomogeneity of the magnetic field, as given by the gradient of the magnetic energy density $D_a\rho_B$. The result is given in Appendix B by Eq. (B.12).

[‡] Note that homogeneous radiation multipoles, i.e. $D_a\tau_{A_\ell} = 0$, imply a Bianchi spacetime to first order [6].

Acknowledgments

CAC was supported by NSERC (at Dalhousie) and NRF (at Cape Town). AAC acknowledges funding from NSERC. CGT was supported by PPARC (at Portsmouth) and NRF (at Cape Town), and thanks Dalhousie University for hospitality while part of this work was done.

Appendix A. The linearized equations

We assume that CDM and baryons share the same 4-velocity, which coincides with that of the fundamental observers. Also, confining ourselves to times after last scattering, we may treat the magnetized dust and the radiation fluid as independently conserved entities (i.e., $\nabla^b T_{ab} = 0 = \nabla^b \mathcal{T}_{ab}$). Then we arrive at the following linearized evolution equations for the magnetised dust (see [8])

$$\dot{\rho}_M + \Theta \rho_M = 0, \quad (A.1)$$

$$\rho_M A_a + \frac{1}{3} D_a \rho_B + \text{div} \Pi_a = 0, \quad (A.2)$$

$$\dot{\rho}_B + \frac{4}{3} \Theta \rho_B = 0, \quad (A.3)$$

$$\dot{\Pi}_{ab} + \frac{4}{3} \Theta \Pi_{ab} = 0, \quad (A.4)$$

and

$$\dot{\mu} + \frac{4}{3} \Theta \mu + \text{div} q = 0, \quad (A.5)$$

$$\dot{q}_a + \frac{4}{3} \Theta q_a + \frac{4}{3} \mu A_a + \frac{1}{3} D_a \mu + \text{div} \pi_a = 0, \quad (A.6)$$

$$\dot{\pi}_{ab} + \frac{4}{3} \Theta \pi_{ab} + \frac{8}{15} \mu \sigma_{ab} + 2 D_{\langle a} q_{b \rangle} + \text{div} \xi_{ab} = 0, \quad (A.7)$$

for the photons (see [10]). Note that in deriving Eq. (A.2) we have used the linear relation $\varepsilon_{abc} B^b \text{curl} B^c = \frac{1}{6} D_a B^2 + D^b \Pi_{ab}$ (recall that $D^a B_a = 0$). To first order, the kinematic evolution is given by

$$\dot{\Theta} + \frac{1}{3} \Theta^2 + \frac{1}{2} (\rho_M + 2\mu + 2\rho_B) - \text{div} A - \Lambda = 0, \quad (A.8)$$

$$\dot{\sigma}_{ab} + \frac{2}{3} \Theta \sigma_{ab} + E_{ab} - \frac{1}{2} \pi_{ab} - \frac{1}{2} \Pi_{ab} - D_{\langle a} A_{b \rangle} = 0, \quad (A.9)$$

$$\dot{\omega}_a + \frac{2}{3} \Theta \omega_a + \frac{1}{2} \text{curl} A_a = 0, \quad (A.10)$$

$$q_a - \frac{2}{3} D_a \Theta + \text{div} \sigma_a - \text{curl} \omega_a = 0, \quad (A.11)$$

$$\text{div} \omega = 0, \quad (A.12)$$

where A_a is given by Eq. (A.2). Finally, the spacetime geometry is determined by [10]

$$\dot{E}_{ab} + \Theta E_{ab} - \text{curl} H_{ab} + \frac{1}{2} (\rho_M + \frac{4}{3} \mu) \sigma_{ab} + \frac{1}{2} \dot{\pi}_{ab} + \frac{1}{6} \Theta \pi_{ab} - \frac{1}{2} \Theta \Pi_{ab} + \frac{1}{2} D_{\langle a} q_{b \rangle} = 0, \quad (A.13)$$

$$\dot{H}_{ab} + \Theta H_{ab} + \text{curl} E_{ab} - \frac{1}{2} \text{curl} \pi_{ab} - \frac{1}{2} \text{curl} \Pi_{ab} = 0, \quad (A.14)$$

$$H_{ab} - \text{curl} \sigma_{ab} - D_{\langle a} \omega_{b \rangle} = 0, \quad (A.15)$$

$$\text{div} E_a + \frac{1}{2} \text{div} \pi_a + \frac{1}{2} \text{div} \Pi_a - \frac{1}{3} D_a (\rho_M + \mu + \rho_B) + \frac{1}{3} \Theta q_a = 0, \quad (A.16)$$

$$\text{div} H_a + \frac{1}{2} \text{curl} q_a - (\rho_M + \frac{4}{3} \mu) \omega_a = 0, \quad (A.17)$$

$$\mathcal{R}_{\langle ab \rangle} + \frac{1}{3} \Theta \sigma_{ab} - \frac{1}{2} \pi_{ab} - \frac{1}{2} \Pi_{ab} - E_{ab} = 0, \quad (A.18)$$

$$\mathcal{R} - 2(\rho_M + \mu + \rho_B) + \frac{2}{3}\Theta^2 - 2\Lambda = 0, \quad (\text{A.19})$$

where \mathcal{R}_{ab} and \mathcal{R} are respectively the projected Ricci tensor and Ricci scalar. To proceed further we now assume that the fluid flow remains geodesic (i.e. $A_a = 0$) despite the magnetic presence. In other words, we impose the force-free condition on the magnetic field (i.e. $\varepsilon_{abc}B^b \text{curl} B^c = 0 = \frac{1}{3}D_a \rho_B + \text{div} \Pi_a$).

Appendix B. Calculating the limits

Our method provides a small refinement of [9], allowing us to get slightly stronger limits (by about a factor of about two). In [9], limits on σ_{ab} were calculated in the following way: First, Eq. (A.7) is solved for σ_{ab} , and then the separate limits in Eqs.(7)–(22) of [9] were inserted to give the following limit:

$$\frac{|\sigma_{ab}|}{\Theta} < \frac{8}{3}\epsilon_2 + \epsilon_2^* + 5\epsilon_1^\dagger + \frac{9}{7}\epsilon_3^\dagger. \quad (\text{B.1})$$

However, if, after solving Eq. (A.7) for σ_{ab} , we use Eq. (41) of [6] to convert $\pi_{ab} \rightarrow \tau_{ab}$ etc. (i.e., $\tau_a \simeq 3q_a/4\mu$, $\tau_{ab} \simeq 15\pi_{ab}/8\mu$...), and then use Eqs. (1)–(4) of [9] (after expanding all derivatives, and using the relevant evolution equations), some terms cancel, and we get the tighter limit:

$$\frac{|\sigma_{ab}|}{\Theta} < \epsilon_2^* + 5\epsilon_1^\dagger + \frac{9}{7}\epsilon_3^\dagger. \quad (\text{B.2})$$

This gives simpler limits than using the method in [9]. As a further example, consider the limits on E_{ab} in the case of no magnetic field (including cosmological constant):

$$\frac{|E_{ab}|}{\Theta} < H \left\{ 10\epsilon_1^\dagger + 15\epsilon_1^{\dagger*} + 2\epsilon_2^* + 3\epsilon_2^{**} + \frac{18}{7}\epsilon_3^\dagger + \frac{27}{7}\epsilon_3^{\dagger*} \right\} + \frac{4}{15}H\Omega_R\epsilon_2, \quad (\text{B.3})$$

which is less than the corresponding limit in Eq. (28), [9].

Appendix B.1. Magnetic field strength

Our first problem is to find limits on Π_{ab} . In the absence of magnetic fields, limits on E_{ab} may be found directly from Eq. (A.9), using Eq. (A.7). However, with magnetic fields present, this will give limits on the combination $|E_{ab} - \frac{1}{2}\Pi_{ab}|$, so we have to find separate equations for E_{ab} and Π_{ab} . We can do this by solving Eq. (A.13) and the time derivative of Eq. (A.9), which gives

$$\begin{aligned} \Pi_{ab} = & -\frac{3}{2\Theta}\ddot{\sigma}_{ab} - \frac{5}{2}\dot{\sigma}_{ab} + \Theta\sigma_{ab} \left(-\frac{2}{3} + 2\frac{\mu}{\Theta^2} + \frac{5}{4}\frac{\rho_M}{\Theta^2} + 2\frac{\rho_B}{\Theta^2} - \frac{\Lambda}{\Theta^2} \right) \\ & + \frac{3}{2\Theta}\dot{\pi}_{ab} + \pi_{ab} + \frac{3}{4\Theta}D_{\langle a}q_{b\rangle} - \frac{3}{2\Theta}\text{curl} H_{ab}, \end{aligned} \quad (\text{B.4})$$

with a similar equation for E_{ab} . We have used Eq. (A.4). In the linear regime, we can drop the angled brackets on time derivatives of PSTF tensors. Decoupling these quantities has introduced extra uncertainty into our equations, in the form of $\ddot{\sigma}_{ab}$. In Eq. (B.4), all the shear terms may be found in terms of the τ_{A_ℓ} simply by taking appropriate derivatives of Eq. (A.7) and using Eqs. (11) and (12), followed by (5). The only term left to worry about is the $\text{curl} H_{ab}$ term; however, we may use D_c of Eq. (A.15), given that

$$|D_c H_{ab}| < |D_a D_b \sigma_{cd}| + |D_a D_b \omega_c|. \quad (\text{B.5})$$

Limits on the second gradient of the shear may be found from Eq. (A.7):

$$|D_a D_b \sigma_{cd}| < \frac{9}{7}H^3 \left\{ 105\epsilon_1^{\dagger\dagger\dagger} + 14\epsilon_2^{\dagger\dagger} + 21\epsilon_2^{\dagger\dagger*} + 27\epsilon_3^{\dagger\dagger\dagger} \right\}. \quad (\text{B.6})$$

The rotation term may be found using $\omega_a = -\text{curl} D_a \mu / 2\dot{\mu} = \varepsilon_{abc} D^b D^c \mu / 8H\mu$ and Eq. (A.6):

$$|D_a D_b \omega_c| < \frac{81}{10}H^3 \left\{ 5\epsilon_1^{\dagger\dagger\dagger} + 5\epsilon_1^{\dagger\dagger\dagger*} + 6\epsilon_2^{\dagger\dagger\dagger\dagger} \right\}. \quad (\text{B.7})$$

So we finally have

$$\begin{aligned} \frac{|\Pi_{ab}|}{\Theta} &< H \left\{ \frac{1}{4} \Omega_M \left[25\epsilon_1^\dagger + 5\epsilon_2^* + \frac{45}{7}\epsilon_3^\dagger \right] \right. \\ &+ \Omega_R \left[9\epsilon_1^\dagger + \frac{8}{15}\epsilon_2 + \frac{6}{5}\epsilon_2^* + \frac{18}{7}\epsilon_3^\dagger \right] + \Omega_\Lambda \left[5\epsilon_1^\dagger + \epsilon_2^* + \frac{9}{7}\epsilon_3^\dagger \right] \\ &+ 10\epsilon_1^\dagger + \frac{75}{2}\epsilon_1^{\dagger*} + \frac{45}{2}\epsilon_1^{\dagger**} + 2\epsilon_2^* + \frac{15}{2}\epsilon_2^{\dagger*} + \frac{9}{2}\epsilon_2^{\dagger**} + \frac{18}{7}\epsilon_3^\dagger + \frac{135}{14}\epsilon_3^{\dagger*} + \frac{81}{14}\epsilon_3^{\dagger**} \\ &\left. + \frac{117}{4}\epsilon_1^{\dagger\dagger\dagger} + \frac{27}{4}\epsilon_1^{\dagger\dagger\dagger*} + 3\epsilon_2^{\dagger\dagger} + \frac{9}{2}\epsilon_2^{\dagger\dagger*} + \frac{81}{10}\epsilon_2^{\dagger\dagger\dagger\dagger} + \frac{81}{14}\epsilon_3^{\dagger\dagger\dagger} \right\}; \end{aligned} \quad (B.8)$$

$$\begin{aligned} \frac{|E_{ab}|}{\Theta} &< H \left\{ \frac{1}{8} \Omega_M \left[25\epsilon_1^\dagger + 5\epsilon_2^* + \frac{45}{7}\epsilon_3^\dagger \right] + \Omega_R \left[\frac{9}{2}\epsilon_1^\dagger + \frac{3}{5}\epsilon_2^* + \frac{9}{7}\epsilon_3^\dagger \right] \right. \\ &+ \frac{1}{2}\Omega_\Lambda \left[5\epsilon_1^\dagger + \epsilon_2^* + \frac{9}{7}\epsilon_3^\dagger \right] \\ &+ 15\epsilon_1^\dagger + \frac{135}{4}\epsilon_1^{\dagger*} + \frac{45}{4}\epsilon_1^{\dagger**} + 3\epsilon_2^* + \frac{27}{4}\epsilon_2^{\dagger*} + \frac{9}{4}\epsilon_2^{\dagger**} + \frac{27}{7}\epsilon_3^\dagger + \frac{243}{28}\epsilon_3^{\dagger*} + \frac{81}{28}\epsilon_3^{\dagger**} \\ &\left. + \frac{117}{8}\epsilon_1^{\dagger\dagger\dagger} + \frac{27}{8}\epsilon_1^{\dagger\dagger\dagger*} + \frac{3}{2}\epsilon_2^{\dagger\dagger} + \frac{9}{4}\epsilon_2^{\dagger\dagger*} + \frac{81}{20}\epsilon_2^{\dagger\dagger\dagger\dagger} + \frac{81}{28}\epsilon_3^{\dagger\dagger\dagger} \right\}. \end{aligned} \quad (B.9)$$

Comparing Eq. (B.9) with the limits found in the absence of a magnetic field, Eq. (B.3), reveals the extra complexity and uncertainty involved in having just one additional field.

Appendix B.2. Inhomogeneity of the field

To find limits on the inhomogeneity, we need to find limits on $D_a \rho_B = -3 \operatorname{div} \Pi_a$. [Note that solving D_a of Eqs. (A.8) and (A.16) for $D_a \rho_B$ does not work since it does not separate gradients of ρ_B and ρ_M .] First we take D^a of Eq. (B.4), and note that

$$\operatorname{div} \operatorname{curl} H_a = \frac{1}{2} \operatorname{curl} \operatorname{div} H_a = -\frac{1}{4} \operatorname{curl} \operatorname{curl} q_a + \frac{1}{2} \left(\rho_M + \frac{4}{3}\mu \right) \operatorname{curl} \omega_a, \quad (B.10)$$

so

$$|\operatorname{div} \operatorname{curl} H_a| < \frac{1}{4} |D_a D_b q| + \frac{1}{2} \left(\rho_M + \frac{4}{3}\mu \right) |D_a \omega_b|. \quad (B.11)$$

Hence we find that

$$\begin{aligned} \frac{|D_a \rho_B|}{H^3} &< \frac{\max |D_a \rho_B|}{H^3} \equiv \Omega_M \left\{ \frac{2511}{4}\epsilon_1^{\dagger\dagger} + \frac{243}{8}\epsilon_1^{\dagger\dagger*} + 54\epsilon_2^\dagger + 162\epsilon_2^{\dagger*} + \frac{729}{20}\epsilon_2^{\dagger\dagger\dagger} + \frac{2187}{14}\epsilon_3^{\dagger\dagger\dagger} \right\} \\ &+ \Omega_\Lambda \left\{ \frac{405}{2}\epsilon_1^{\dagger\dagger} + 81\epsilon_2^\dagger + \frac{243}{2}\epsilon_2^{\dagger*} + \frac{729}{14}\epsilon_3^{\dagger\dagger} \right\} \\ &+ \Omega_R \left\{ 972\epsilon_1^{\dagger\dagger} + \frac{81}{2}\epsilon_1^{\dagger\dagger*} + \frac{513}{5}\epsilon_2^\dagger + \frac{2187}{10}\epsilon_2^{\dagger*} + \frac{243}{5}\epsilon_2^{\dagger\dagger\dagger} + \frac{3645}{14}\epsilon_3^{\dagger\dagger} \right\} \\ &+ \frac{3645}{2}\epsilon_1^{\dagger\dagger} + \frac{8505}{2}\epsilon_1^{\dagger\dagger*} + \frac{3645}{2}\epsilon_1^{\dagger\dagger**} + 54\epsilon_2^\dagger + 567\epsilon_2^{\dagger*} + 972\epsilon_2^{\dagger**} \\ &+ \frac{729}{2}\epsilon_2^{\dagger***} + \frac{6561}{14}\epsilon_3^{\dagger\dagger} + \frac{2187}{2}\epsilon_3^{\dagger\dagger*} + \frac{6561}{14}\epsilon_3^{\dagger\dagger**}. \end{aligned} \quad (B.12)$$

- [1] D. Grasso and H.R. Rubinstein (2001) *Phys. Rep.* **348**, 163; L. Widrow (2002) *astro-ph/0207240*.
- [2] J.D. Barrow, P.G. Ferreira, and J. Silk (1997) *Phys. Rev. Lett.* **78**, 3610.
- [3] R. Maartens, G.F.R. Ellis and W.R. Stoeger (1996) *Astron. Astrophys.* **309**, L7.
- [4] C.A. Clarkson and A.A. Coley (2001) *Class. Quantum Grav.* **18**, 1305.
- [5] W.R. Stoeger, R. Maartens, and G.F.R. Ellis (1995) *Astrophys. J.* **443**, 1.
- [6] R. Maartens, G.F.R. Ellis and W.R. Stoeger (1995) *Phys. Rev. D* **51**, 1525.
- [7] A.D. Challinor and A.N. Lasenby (1998) *Phys. Rev. D* **58**, 023001.
- [8] C.G. Tsagas and J.D. Barrow (1997) *Class. Quantum Grav.* **14**, 2539; *ibid.*, (1998) **15**, 3523; C.G. Tsagas and R. Maartens (2000) *Phys. Rev. D* **61**, 083519.
- [9] R. Maartens, G.F.R. Ellis and W.R. Stoeger (1995) *Phys. Rev. D* **51**, 5942.
- [10] R. Maartens, T. Gebbie and G.F.R. Ellis (1999) *Phys. Rev. D* **59**, 083506.
- [11] W.R. Stoeger, M.E. Araujo and T. Gebbie (1999) *Astrophys. J.* **476**, 435.